

## Supplementary Materials

### Spin Cross-Over (SCO) complex based on unsymmetrical functionalized triazacyclononane ligand: structural characterization and magnetic properties

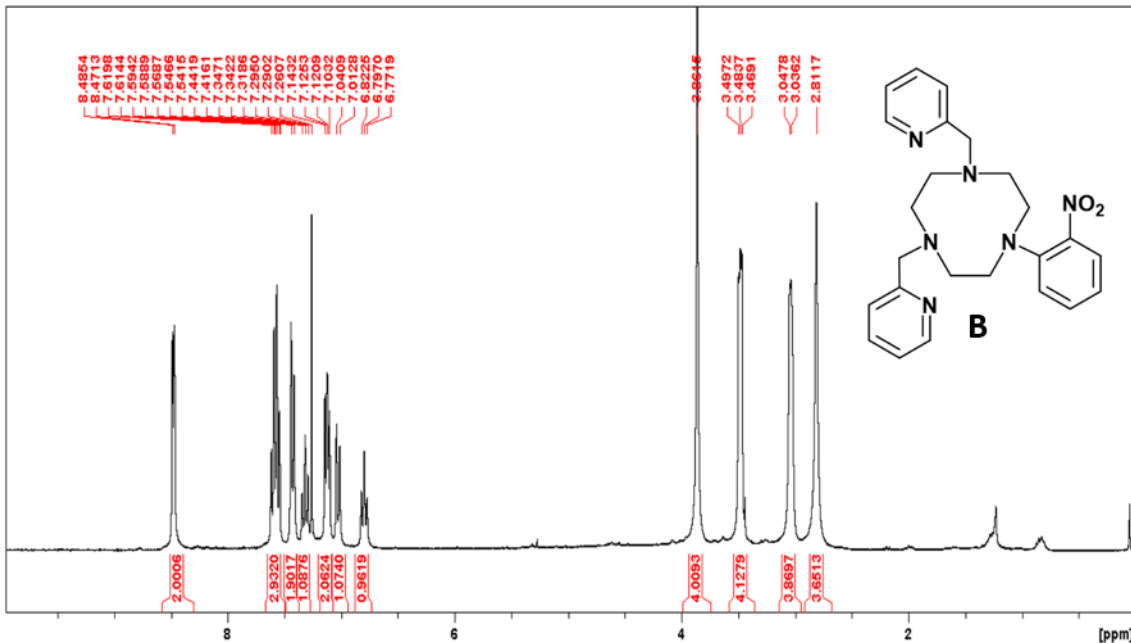


Figure S1. <sup>1</sup>H NMR spectrum of compound B (CDCl<sub>3</sub>, 300 MHz, 25°C)

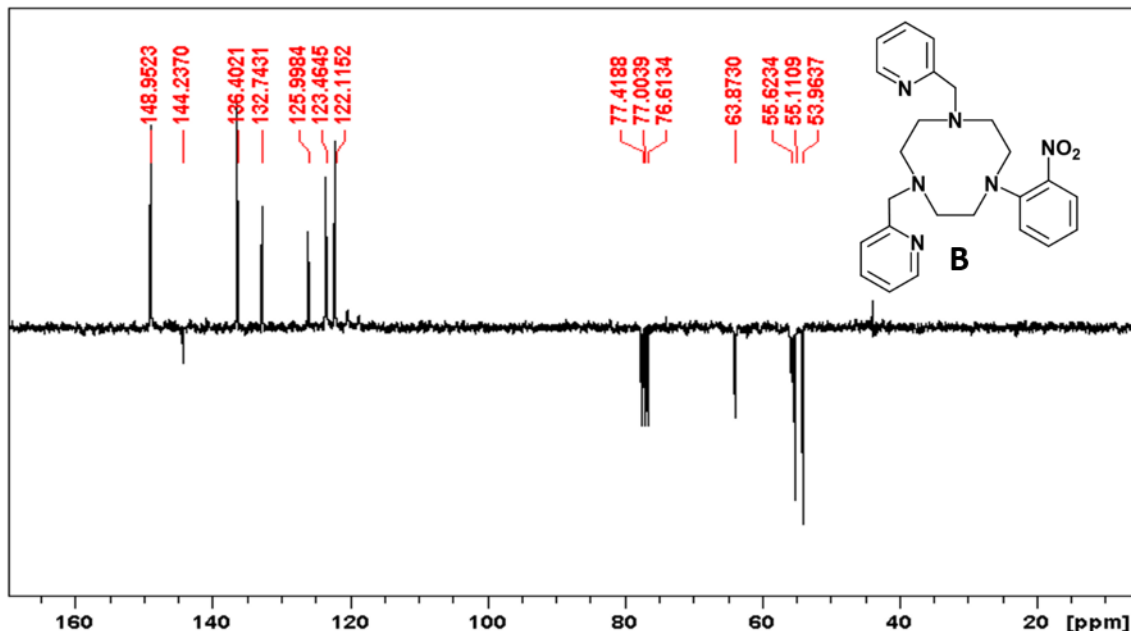
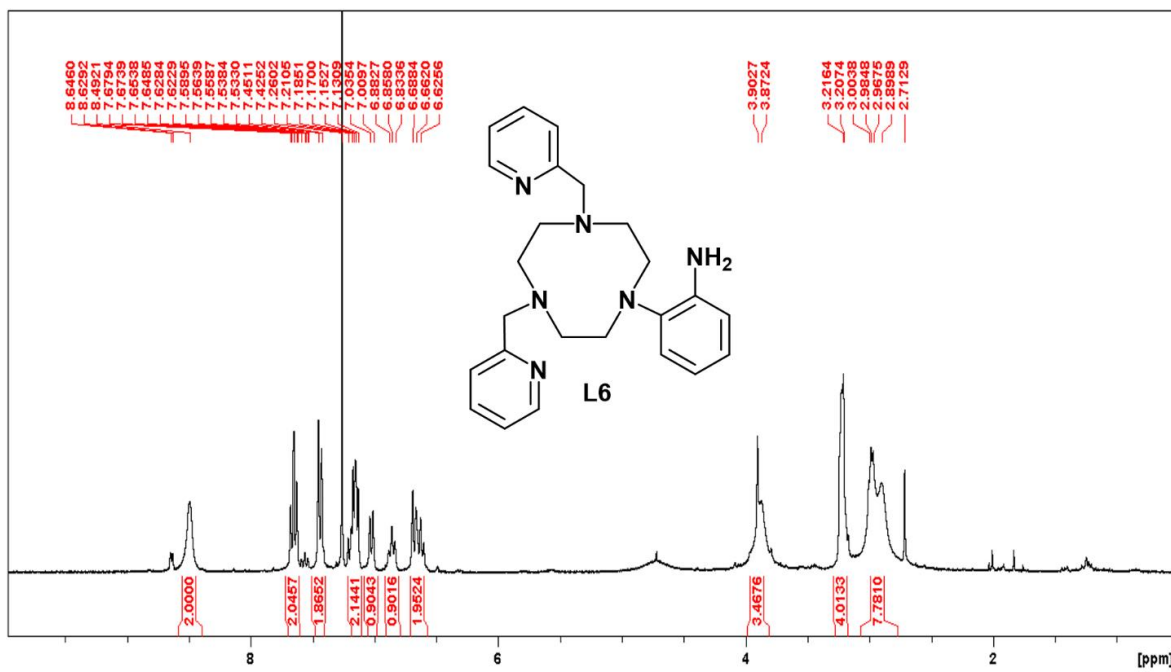
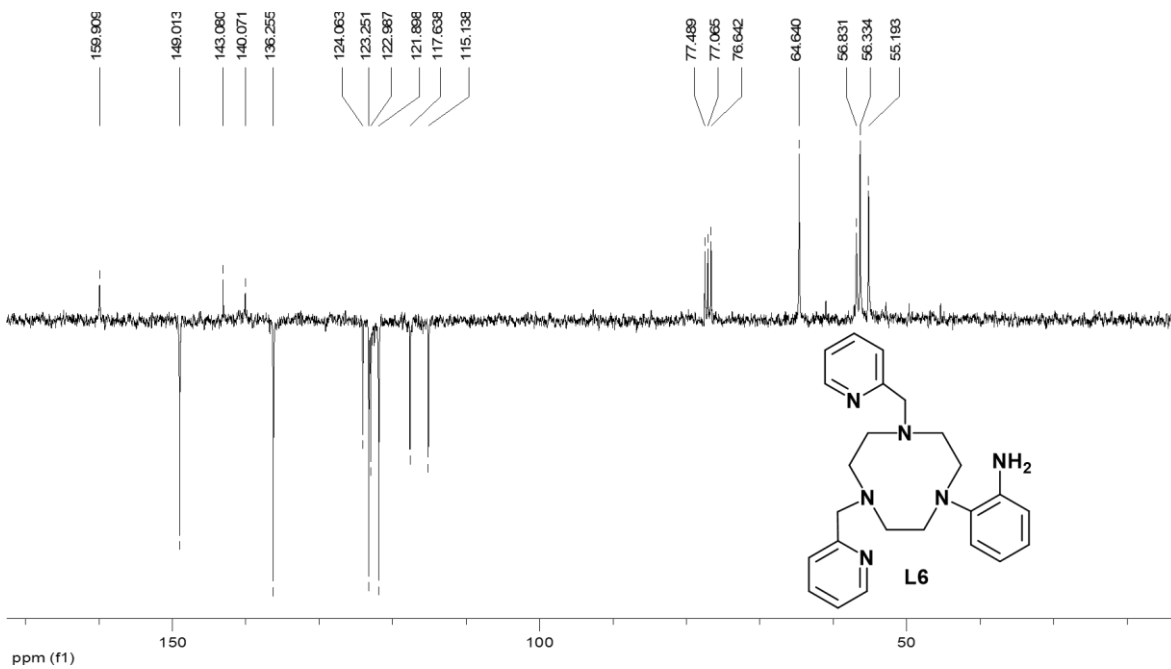


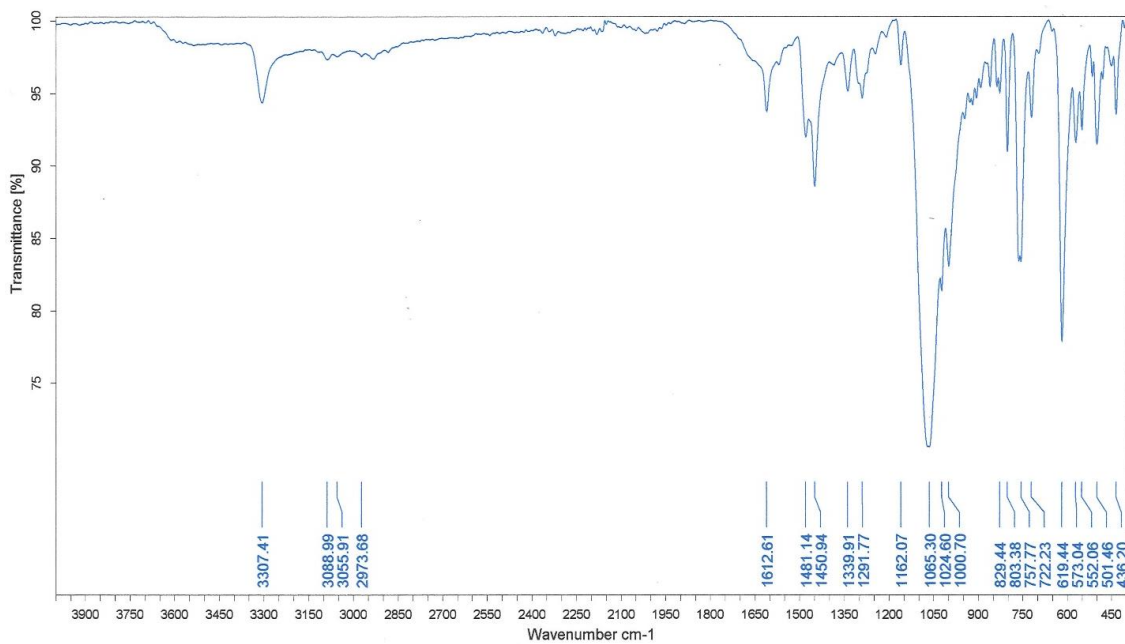
Figure S2. <sup>13</sup>C NMR spectrum of compound B (CDCl<sub>3</sub>, 75.4 MHz, 25°C)



**Figure S3.** <sup>1</sup>H NMR spectrum of compound L6 (CDCl<sub>3</sub>, 300 MHz, 25°C)



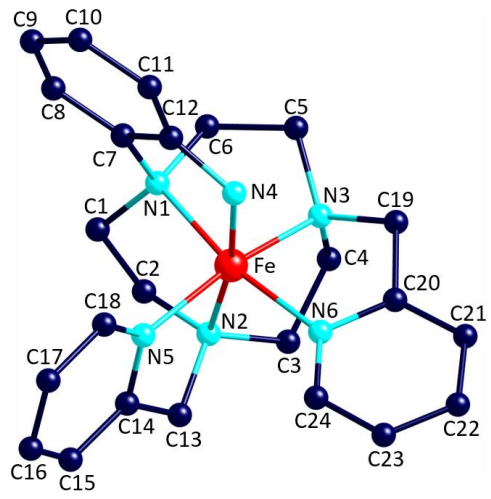
**Figure S4.** <sup>13</sup>C NMR spectrum of compound L6 (CDCl<sub>3</sub>, 75.4 MHz, 25°C)



**Figure S5.** IR data ( $\nu/\text{cm}^{-1}$ ) spectrum of complex  $[\text{Fe}(\text{L6})](\text{ClO}_4)_2$  (**1**): 3307(w), 1613(w), 1481(m), 1451(m), 1340(w), 1292(w), 1162(w), 1065(s), 1001(br), 829(w), 803(m), 758(s), 722(w), 619(s), 573(w), 552(w), 501(m), 436w).

Table S1. Selected bond distances ( $\text{\AA}$ ) for complex **1** (see Figure S6 for the atom labelling scheme)

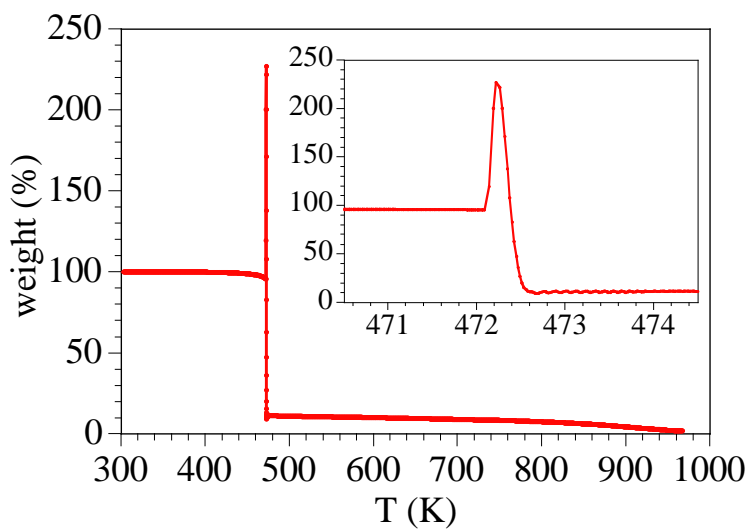
Fe-N(1)	2.002(5)	C(10)-C(11)	1.381(10)
Fe-N(2)	1.998(5)	C(11)-C(12)	1.384(9)
Fe-N(3)	1.999(4)	C(12)-N(1)	1.461(8)
Fe-N(4)	2.005(5)	C(13)-N(2)	1.490(7)
Fe-N(5)	1.999(4)	C(13)-C(14)	1.506(8)
Fe-N(6)	1.973(5)	C(14)-N(5)	1.349(7)
C(1)-N(1)	1.491(9)	C(14)-C(15)	1.390(8)
C(1)-C(2)	1.505(10)	C(15)-C(16)	1.403(9)
C(2)-N(2)	1.501(9)	C(16)-C(17)	1.378(9)
C(3)-C(4)	1.490(9)	C(17)-C(18)	1.378(7)
C(3)-N(2)	1.513(8)	C(18)-N(5)	1.342(7)
C(4)-N(3)	1.507(10)	C(19)-N(3)	1.466(11)
C(5)-C(6)	1.502(11)	C(19)-C(20)	1.518(10)
C(5)-N(3)	1.506(8)	C(20)-N(6)	1.350(7)
C(6)-N(1)	1.517(7)	C(20)-C(21)	1.404(10)
C(7)-C(12)	1.375(10)	C(21)-C(22)	1.359(11)
C(7)-C(8)	1.409(9)	C(22)-C(23)	1.365(9)
C(7)-N(4)	1.466(8)	C(23)-C(24)	1.352(9)
C(8)-C(9)	1.411(9)	C(24)-N(6)	1.362(7)
C(9)-C(10)	1.373(10)		



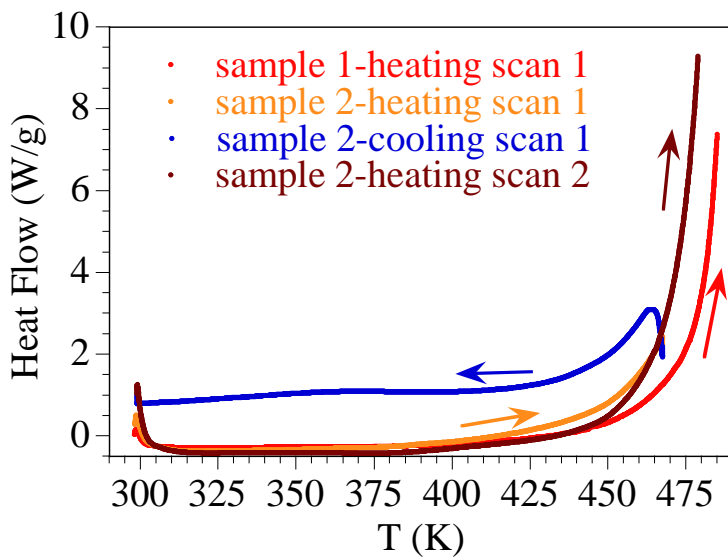
**Figure S6.** Structure of cationic complex of **1** showing the atom labelling scheme and the coordination environment of the  $\text{Fe}(\text{II})$  ion.

Table S2. Selected bond angles ( $^{\circ}$ ) for complex **1** (see Figure S6 for the atom labelling scheme)

N(6)-Fe-N(2)	98.58(19)	C(7)-C(12)-N(1)	115.4(6)
N(6)-Fe-N(5)	94.76(17)	C(11)-C(12)-N(1)	124.8(7)
N(2)-Fe-N(5)	82.90(17)	N(2)-C(13)-C(14)	108.4(5)
N(6)-Fe-N(1)	168.49(17)	N(5)-C(14)-C(15)	122.8(6)
N(2)-Fe-N(1)	86.4(2)	N(5)-C(14)-C(13)	116.1(5)
N(5)-Fe-N(1)	96.14(17)	C(15)-C(14)-C(13)	121.0(6)
N(6)-Fe-N(3)	84.1(2)	C(14)-C(15)-C(16)	117.7(6)
N(2)-Fe-N(3)	85.6(2)	C(16)-C(17)-C(18)	118.7(6)
N(5)-Fe-N(3)	168.2(2)	N(5)-C(18)-C(17)	123.2(6)
N(1)-Fe-N(3)	86.0(2)	N(3)-C(19)-C(20)	111.2(6)
N(6)-Fe-N(4)	91.28(19)	N(6)-C(20)-C(21)	121.3(7)
N(2)-Fe-N(4)	170.00(19)	N(6)-C(20)-C(19)	114.1(6)
N(5)-Fe-N(4)	94.66(17)	C(21)-C(20)-C(19)	124.5(6)
N(1)-Fe-N(4)	84.2(2)	C(22)-C(21)-C(20)	119.8(7)
N(3)-Fe-N(4)	97.2(2)	C(21)-C(22)-C(23)	118.4(7)
N(1)-C(1)-C(2)	108.7(6)	C(24)-C(23)-C(22)	120.9(7)
N(2)-C(2)-C(1)	111.4(6)	C(23)-C(24)-N(6)	122.3(6)
C(4)-C(3)-N(2)	109.1(5)	C(12)-N(1)-C(1)	114.2(5)
C(3)-C(4)-N(3)	110.6(5)	C(12)-N(1)-C(6)	110.2(5)
C(6)-C(5)-N(3)	107.8(6)	C(1)-N(1)-C(6)	110.1(6)
C(5)-C(6)-N(1)	110.4(6)	C(13)-N(2)-C(2)	111.0(6)
C(12)-C(7)-C(8)	121.3(6)	C(13)-N(2)-C(3)	110.7(5)
C(12)-C(7)-N(4)	117.4(6)	C(2)-N(2)-C(3)	112.6(5)
C(8)-C(7)-N(4)	121.2(7)	C(19)-N(3)-C(5)	111.6(6)
C(7)-C(8)-C(9)	117.8(7)	C(19)-N(3)-C(4)	111.2(6)
C(10)-C(9)-C(8)	120.1(7)	C(5)-N(3)-C(4)	110.8(6)
C(9)-C(10)-C(11)	121.0(7)	C(18)-N(5)-C(14)	118.1(5)
C(10)-C(11)-C(12)	120.1(8)	C(20)-N(6)-C(24)	117.4(6)
C(7)-C(12)-C(11)	119.7(7)		



**Figure S7.** Thermogravimetric measurements of compound **1** at a heating rate of 10 K/min in the temperature range 300–980 K. Inset shows a zoom of the decomposition peak at *ca.* 472 K.



**Figure S8.** DSC scans for two different samples of compound **1** for different heating and cooling scans at a scan rate of 10 K/min.

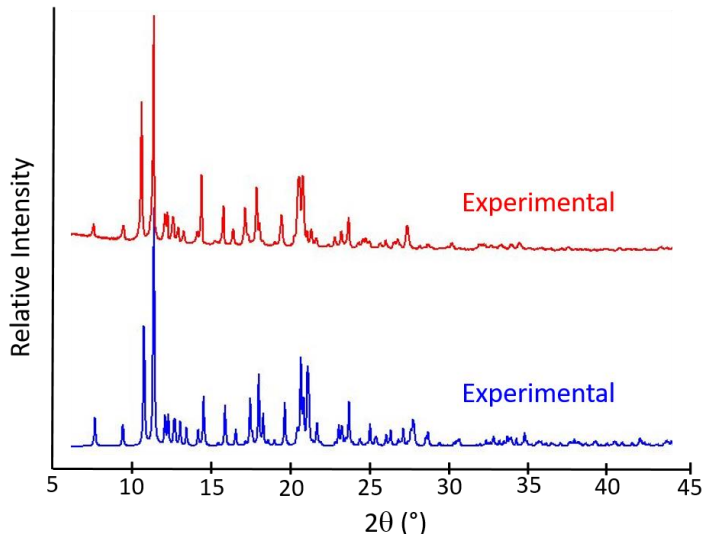


**Figure S9.** Observed and calculated X-ray powder diffraction patterns for complex **1**